

Field data based real-time parameter identification of 3D shear building models

J. Mauricio Angeles-Cervantes[†] and Luis Alvarez-Icaza[‡]

Abstract—A re-parameterization of a least squares algorithm proposed for identifying the parameters of 3D shear models is tested with non-processed data from instrumented buildings. The linear shear building models consider seismic excitation in two orthogonal directions and three degrees of freedom for each story. This new parameterization allows a very important reduction on the number of calculations involved. The performance of the method confirms the possibility of real-time 3D parameter recovering.

Index Terms—building vibration control, parameter identification, least-squares identification

I. INTRODUCTION

Application of advanced control techniques to real-time building vibration control is becoming more important in regions subject to seismic hazard¹. It is common that the parameters used for building design are different from the real ones, due to the natural uncertainties in any construction process. From a practical point of view this is not a problem, as the use of safety factors guarantees that structures will resist predicted forces. From a control point of view, however, it is best to have a mathematical model of the building that accurately predicts its real dynamic behavior.

Identification methods are useful for recovering the parameters of buildings' dynamic models without destructive testing; it is only necessary to excite the structure and measure its behavior. If the excitation is an earthquake, then identification can be executed in real-time and in parallel with control actions. Although there is a good body of work related with the identification of building model parameters, (see, for example, [2], [3], [4], [5]), most of it refers to planar building models and it is realized off-line. The work related with real-time identification of more than one degree of freedom (DOF) per story is scarce, even though it is well known that torsional effects are important for structures with non-symmetric stiffness [6], [7], [8].

In [9], authors propose a modified least-square identification algorithm to recover the model parameters of a building seismically excited with two horizontal and orthogonal components, using for that purpose acceleration measurements. The algorithm is numerically efficient and can be applied to non-symmetrical buildings whose construction is based on planar frames. This work was extended in [10]

to allow acceleration sensors to be arbitrarily placed on the building stories. This paper extends the results obtained in [9], [10] in two important directions. First, the case when acceleration measurements are only available for a limited number of structure stories is now considered. This issue is related with model reduction, as most buildings have limited instrumentation, and it is important that the obtained parameters from the reduced model preserve key features of the dynamic behavior for the full structure. Second, the algorithm is tested with data obtained from two instrumented buildings that were taken during an earthquake. Testing the algorithm proposed in [9] and [10] with non-processed field data is very important to observe the effect of noisy measurements in the parameter estimation.

The rest of the paper contains several sections that deal with the building's mathematical model, sensor location and the least-squares algorithm. Identification results with field data obtained from instrumented building and concluding remarks are also included.

II. MATHEMATICAL MODEL

The 3D shear model of a building based on planar frames under the assumption of rigid diaphragm has two displacement coordinates and one torsion coordinate for each story. The reference system for each story is located at its center of mass. Fig. 1 shows an equivalent diagram and indicates the three DOF for each story. It also shows, in the right hand side, one possible arrangement of sensors in the rigid diaphragm of each story. Longitudinal displacements are tagged as x and y and rotation about the vertical axis as θ . The elastic model for this building is of the form

$$M\ddot{U} + C\dot{U} + KU = -M\ddot{U}_g, \quad (1)$$

where $U, \dot{U}, \ddot{U} \in \mathcal{R}^{3n}$ are the displacement, velocity and acceleration vectors, respectively, for each of the n stories in the three directions of motion considered x, y and $\theta \in \mathcal{R}^n$. $M = M^T > 0$, $C = C^T \geq 0$ and $K = K^T > 0$ are the inertia, damping and stiffness matrices, respectively. Finally, \ddot{U}_g is the acceleration vector of the ground, that in this case only considers excitation in x and y directions. Details about these matrices for buildings constructed with planar frames can be found in [9]. Although the form of the model in Eq. (1) is very standard, torsional parameters are very difficult to calculate for buildings with non-symmetric stories.

If conventional accelerometers that measure only in one axis are used, then it is necessary at least to have three

Research sponsored by grants CONACYT 47583 and UNAM-DGAPA-PAPIIT IN109306.

[†]Graduate student, conejo1978@yahoo.com.mx .

[‡]Professor, corresponding author, alvar@pumas.iingen.unam.mx.

Authors are with Instituto de Ingeniería, Universidad Nacional Autónoma de México; 04510 Coyoacán DF, México.

¹See [1] and references therein.

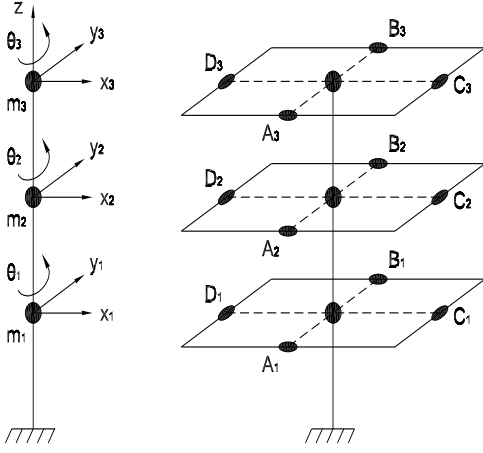


Fig. 1. Scheme of an instrumented building.

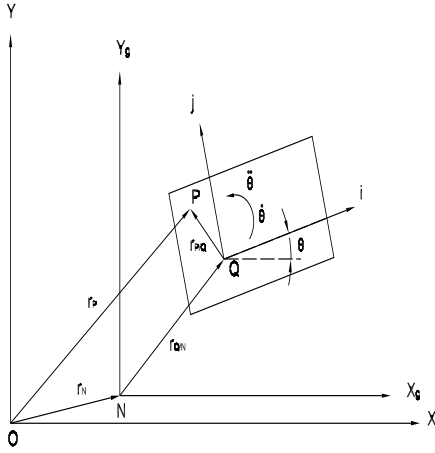


Fig. 2. Scheme of motion.

sensors per story: two in one direction and another in the orthogonal direction. The two parallel measurements are used to obtain the rotational variables: θ , $\dot{\theta}$ and $\ddot{\theta}$. Fig. 2 shows the diaphragm motion on the plane, that results from the composition of the ground motion with respect to an inertial frame (with origin in point O) and a general planar movement of the diaphragm with respect to the ground, N . The absolute position of point P is given by

$$r_P = r_N + r_{Q/N} + r_{P/Q}, \quad (2)$$

where $r_{Q/N}$ is the vector of point Q with respect to point N , and $r_{P/Q}$ is the vector of point P with respect to point Q . To obtain velocity and acceleration of point P , Eq. (2) is derived with respect to time to obtain

$$\dot{r}_P = \dot{r}_N + \dot{r}_{Q/N} + \dot{r}_{P/Q} + \dot{\theta} \times r_{P/Q} \quad (3a)$$

$$\ddot{r}_P = \ddot{r}_N + \ddot{r}_{Q/N} + \ddot{r}_{P/Q} + \dot{\theta} \times (\dot{\theta} \times r_{P/Q}) + \ddot{\theta} \times r_{P/Q} + 2 \dot{\theta} \times \dot{r}_{P/Q} \quad (3b)$$

where $\dot{\theta} \times r_{P/Q}$ is the tangential velocity, $\dot{\theta} \times (\dot{\theta} \times r_{P/Q})$ is the normal acceleration, $\ddot{\theta} \times r_{P/Q}$ is the tangential acceleration

and $2 \dot{\theta} \times \dot{r}_{P/Q}$ represents the Coriolis acceleration. Because of the rigid diaphragm hypothesis, the relative position of any point P with respect to point Q is constant, therefore, $\dot{r}_{P/Q} = 0$ and $\ddot{r}_{P/Q} = 0$, and the absolute velocity and acceleration of point P are

$$\dot{r}_P = \dot{r}_N + \dot{r}_{Q/N} + \dot{r}_{P/Q} + \dot{\theta} \times r_{P/Q} \quad (4a)$$

$$\ddot{r}_P = \ddot{r}_N + \ddot{r}_{Q/N} + \dot{\theta} \times (\dot{\theta} \times r_{P/Q}) + \ddot{\theta} \times r_{P/Q} \quad (4b)$$

Rotational variables θ , $\dot{\theta}$, $\ddot{\theta}$ are recovered by writing separately coordinates x and y in Eqs. (2) and (4) and applying trigonometrical relations to yield²

$$\text{sen}\theta = \frac{x_A - x_B}{y_{B/A}}, \quad (5a)$$

$$\dot{\theta} = \frac{\dot{x}_A - \dot{x}_B}{y_{B/A} \cos\theta}, \quad (5b)$$

$$\ddot{\theta} = \frac{\ddot{x}_A - \ddot{x}_B + \dot{\theta}^2 y_{B/A} \text{sen}\theta}{y_{B/A} \cos\theta}. \quad (5c)$$

III. LEAST SQUARES IDENTIFICATION

A recursive least-squares algorithm with normalization and forgetting factor is used for recovering the parameters [11] with a convenient reparameterization that allows an important reduction in the order of the covariance matrix [9]. From Eq. (1)

$$\begin{aligned} Z &= \ddot{U} + \ddot{U}_g \in \mathcal{R}^{3n \times 1}, \\ \Phi &= [M^{-1}K \quad M^{-1}C] \in \mathcal{R}^{3n \times 6n}, \\ \Upsilon &= [-U \quad -\dot{U}]^T \in \mathcal{R}^{6n \times 1}, \end{aligned}$$

where n is the number of stories and Φ is the real parameters matrix such that

$$Z = \Phi \Upsilon. \quad (6)$$

Let $\hat{\Phi}$ be the estimated parameters of system 1, such that

$$\hat{Z} = \hat{\Phi} \Upsilon, \quad (7)$$

then the algorithm given by

$$\dot{P} = \delta P - P \frac{\Upsilon \Upsilon^T}{h^2} P, \quad (8)$$

$$\dot{\hat{\Phi}}^T = P \Upsilon \varepsilon^T, \quad (9)$$

where $P = P^T > 0 \in \mathcal{R}^{6n \times 6n}$ is the covariance matrix, $P(0) > 0$, $\delta \geq 0 \in \mathcal{R}$ is the forgetting factor and $h = 1 + \Upsilon^T \Upsilon \in \mathcal{R}$ satisfying $\Upsilon/h \in \mathcal{L}_\infty$, guarantees that the output estimation error

$$\varepsilon = \frac{Z - \hat{Z}}{h^2} \rightarrow 0 \quad \text{where } t \rightarrow \infty.$$

Note that, converse to the standard least squares formulation, in Eq. (6) a matrix of parameters and a regressor vector are used. This allows to reduce the size of the covariance matrix from $P \in \mathcal{R}^{18n^2 \times 18n^2}$ to $P \in \mathcal{R}^{6n \times 6n}$. The regressor vector is reduced from $\Upsilon \in \mathcal{R}^{3n \times 18n^2}$ to $\Upsilon \in \mathcal{R}^{3n \times 6n}$. This size reduction is critical for the algorithm to be executed in real time.

The proof of algorithm convergence can be found in [9].

²A detailed derivation is included in [10].

IV. TORSION CENTER RECOVERY

An important hypothesis to verify in this research was related to torsion center recovering for each story, using for that purpose the parameters obtained as a result of the identification. Assuming that the mass of one story is known, then it is possible to recover the stiffness matrix. The structure of this matrix is

$$K = \begin{bmatrix} k_{xx} & k_{xy} & k_{x\theta} \\ k_{yx} & k_{yy} & k_{y\theta} \\ k_{\theta x} & k_{\theta y} & k_{\theta\theta} \end{bmatrix} \in \mathcal{R}^{3n \times 3n}, \quad K = K^T > 0, \quad (10)$$

Using Eq. (10), the coordinates of the center of torsion for all stories can be computed using the following equation [8]

$$x_{ct} = F_y^{-1} \left\{ k_{\theta x} [k_{yx} - k_{yy} k_{xy}^{-1} k_{xx}]^{-1} + \right. \quad (11a)$$

$$\left. k_{\theta y} \left[-k_{xy}^{-1} k_{xx} (k_{yx} - k_{yy} k_{xy}^{-1} k_{xx})^{-1} \right] \right\} F_y,$$

$$y_{ct} = -F_x^{-1} \left\{ k_{\theta y} [k_{xy} - k_{xx} k_{yx}^{-1} k_{yy}]^{-1} + \right. \quad (11b)$$

$$\left. k_{\theta x} \left[-k_{yx}^{-1} k_{yy} (k_{xy} - k_{xx} k_{yx}^{-1} k_{yy})^{-1} \right] \right\} F_x,$$

where F_x y F_y are arbitrary test loads, that in this case are taken as unit forces.

This calculation is independent of the precise knowledge of the mass that was assumed known. A detailed analysis of Eq. (11) shows that the value of the center of torsion does not change when the stiffness matrices included in the equation are premultiplied and postmultiplied by a non-singular diagonal positive definite matrix, as it is the case of the matrix of masses. This result was corroborated by simulations in [10].

V. SIMULATION RESULTS WITH REDUCED MEASUREMENTS AVAILABILITY

For testing the algorithm in Eqs. (8) and (9), a six-story building was simulated. Two cases were simulated. In the first one, all the stories were equipped with accelerometers, while in the second, only acceleration measurements from the first, second and last story were available. The aim of the second test was to show that, for the model identified in the reduced measurement case, it was possible to recover the most significant vibration frequencies of the building. This approach has a similar goal that what it is pursued when the ‘‘condensation method’’ is used [6]. Fig. 3 shows a scheme of the building with complete and reduced instrumentation, under the assumption that there are three acceleration measurements for each story.

Fig. 4 shows the output estimation error norm for the six-story building for the cases of full and reduced measurements, respectively. Note that for the full measurement case, the output estimation error approaches zero in finite time, implying that the estimated output \hat{Z} is equal to the real output Z . Parameters converge to their real value in a finite

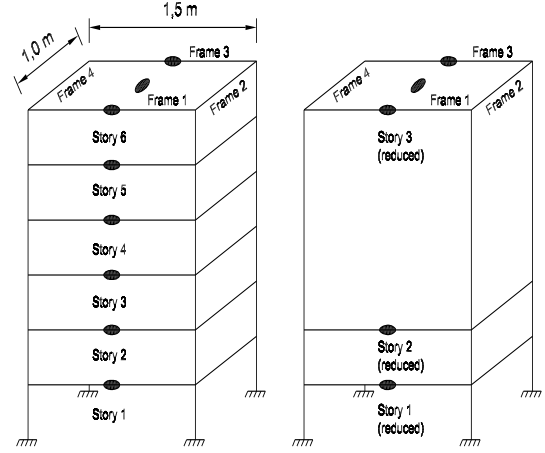


Fig. 3. Building scheme with complete and reduced measurements.

time, as it is shown in Fig. 5, that illustrates the case of two parameters time evolution.

For the case of reduced measurements (Fig. 4.b), it can be noted that the output estimation error does not converge to zero, although it remains within small bounds. This happens because the output measurement contains information about vibration modes that can not be described with the reduced model. This is clear if the last part of the plot in Fig. 4.b is analyzed. At about 43 s there is a change in the characteristics of the ground motion that excites again the identification process. This change has no effect in the full measurement case, that properly identifies the parameters, and has some effect on the reduced measurement case. It should be noted, however, that the size of the output estimation error is relatively small, even when the ground motion changes. Nevertheless, with this reduced model it is possible to recover the most significant natural frequencies of the building. Table I, shows the real and estimated frequencies for the building after 50 seconds of identification. It can be observed that the match is very good for the full measurement case, as expected from previous results [10]. For the reduced measurement case, the match is excellent for the first five natural frequencies and there is a small error for the sixth frequency. The other three frequencies do not correctly match those of the building. It is important to mention that identifying the first three natural frequencies is considered enough, from a civil engineering point of view, and to remark that the identified parameters for the reduced measurement case are different from the parameters of the full measurement case, so there is no reference value for them in the plots.

VI. IDENTIFICATION RESULTS FROM INSTRUMENTED BUILDINGS

To verify the identification algorithm performance beyond simulated buildings, records from two instrumented buildings in Los Angeles, California were used. The first building is a 54-story office building and the second a 7-story hospital building. Records consisted of acceleration measurements

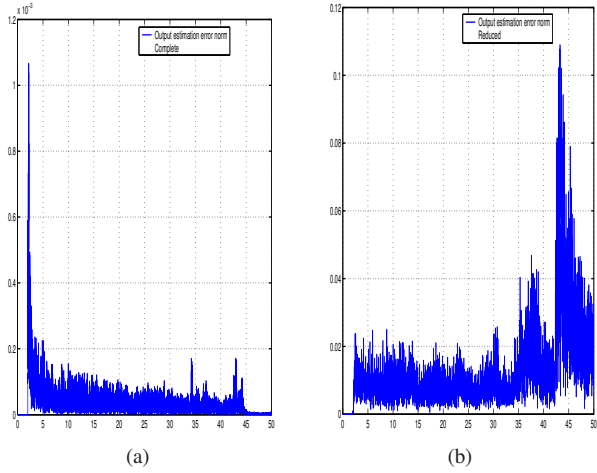


Fig. 4. Output estimation error norm, full measurements case. (a) full measurements case. (b) reduced measurements case.

TABLE I
REAL AND ESTIMATED FREQUENCIES [rad/s]

real	estimated	
	full	reduced
12,815	12,815	12,815
12,867	12,867	12,846
22,295	22,295	22,294
38,367	38,367	38,053
39,203	39,203	39,101
61,158	61,158	65,565
61,512	61,512	73,398
67,669	67,668	77,237
80,311	80,310	123,500
81,393	81,392	
94,205	94,189	
95,206	95,197	
104,38	102,700	
106,28	104,530	

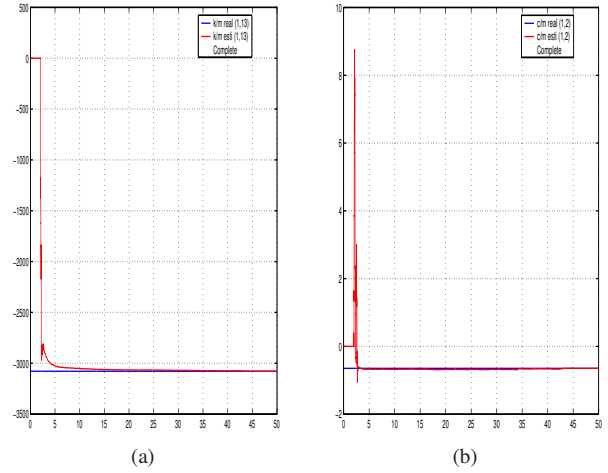


Fig. 5. Time evolution of parameters for the full measurement case. (a) element $(M^{-1}K)_{1,13}$. (b) element $(M^{-1}C)_{1,2}$.

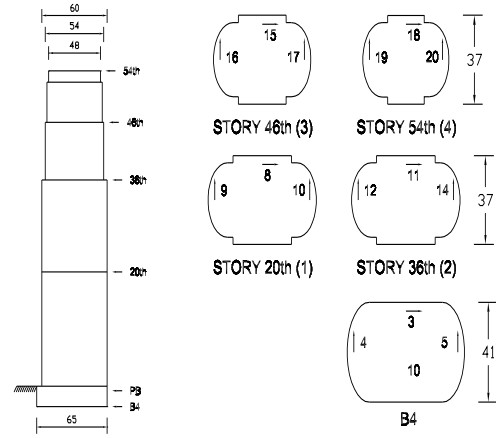


Fig. 6. Scheme of 54-story office building (dimensions in m).

of selected building stories taken during the Northridge earthquake on January 1994 [12]. Acceleration records were integrated off-line to produce velocity and displacement records. As the number of instrumented stories is smaller than the number of stories in both buildings, identification corresponds to reduced measurements availability in both cases.

Fig. 6 shows a scheme of the 54-story building. It has four instrumented stories: 20th, 36th, 46th, and 54th, with two accelerometers in one coordinate and another in the orthogonal coordinate for each one of these stories. There were two additional measurements at the basement that were used as ground acceleration during the earthquake. Therefore, the building was reduced to a four stories building for identification purposes. The output estimation error norm, $\|\varepsilon\|_2$, obtained after applying the identification algorithm in Eqs. (8) and (9) is shown in Fig. 7. It can be observed that error decreases with time. Fig. 8 shows the measured and estimated accelerations for the three DOF of the 3th reduced story (46th real story). The difference between two curves can not be appreciated.

Fig. 9 shows two examples of parameters identification time evolution. The first one corresponds to a stiffness parameter and other to a damping parameter.

Finally, Table II contains the location of the identified torsion centers for the 54th stories office building. The origin of the coordinate reference systems was at the geometric center of each story. The identification algorithm places the torsion centers of this symmetrical building just a few millimeters away of its ideal center position.

TABLE II
54-STORY BUILDING. TORSION CENTER ESTIMATION.

Story	Coordinate x	Coordinate y
1 (20th)	0.002881	0.00010074
2 (36th)	0.0018028	0.0043115
3 (46th)	0.0075868	-0.0065229
4 (54th)	0.0042167	0.0024028

Fig. 10 shows a scheme of the hospital building. Although it has seven stories, only three of them are completely instrumented with two accelerometers in the y direction and another in the x direction. This building is considered as a 3-

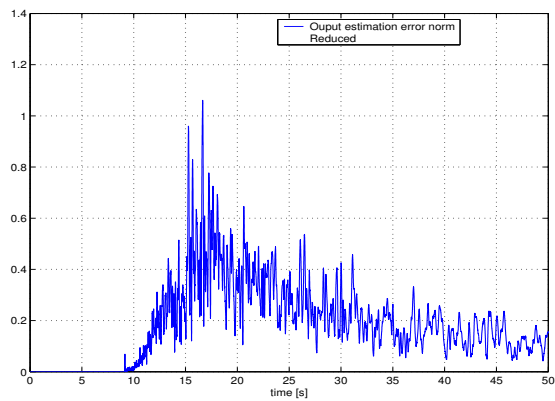


Fig. 7. 54-story building. Output error norm: $\|\varepsilon\|_2$

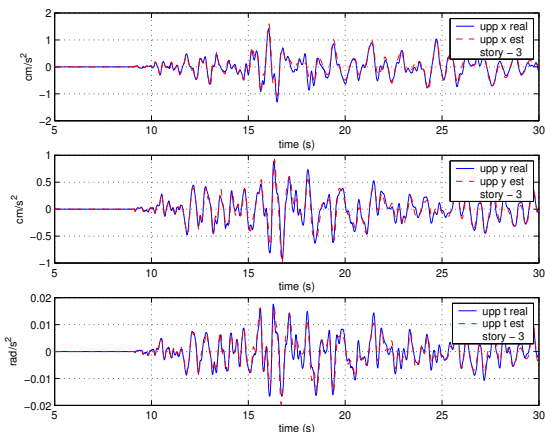


Fig. 8. 54-story building. Measured and estimated accelerations of 3th reduced story (46th real story).

story building for identification purposes. Fig. 11 shows the hospital output estimation error norm obtained after applying the identification algorithm in Eqs. (8) and (9). Note that this error also decreases with time, confirming asymptotic stability of output estimation errors [9].

Fig. 12 shows the measured and estimated accelerations, for the three DOF of the first reduced story of the hospital building. Tracking is very good. Fig. 13 shows two examples of parameter identification time evolution. Table III contains the estimated torsion center. Reference of the coordinate system is illustrated in Fig. 10. Again in this case, the torsion center estimation is properly placed.

TABLE III
HOSPITAL BUILDING. TORSION CENTER ESTIMATION

Story	Coordinate x	Coordinate y
1 (4th)	0.00018689	0
2 (6th)	0.0019449	-0.001631
3 (7th)	0.0044356	-0.002464

Table IV contains the estimated natural frequencies for the 54th stories office building and hospital building.

It is convenient to recall that for this field data there is no reference value for the parameters. There is not, also, a direct

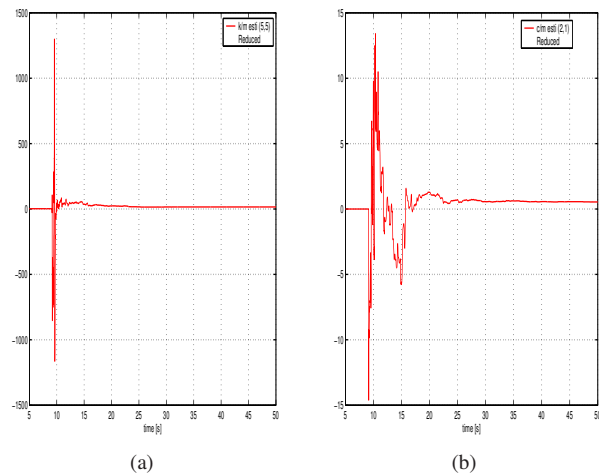


Fig. 9. 54th stories building. Time evolution of parameters. (a) element $(M^{-1}K)_{5,5}$. (b) element $(M^{-1}C)_{2,1}$.

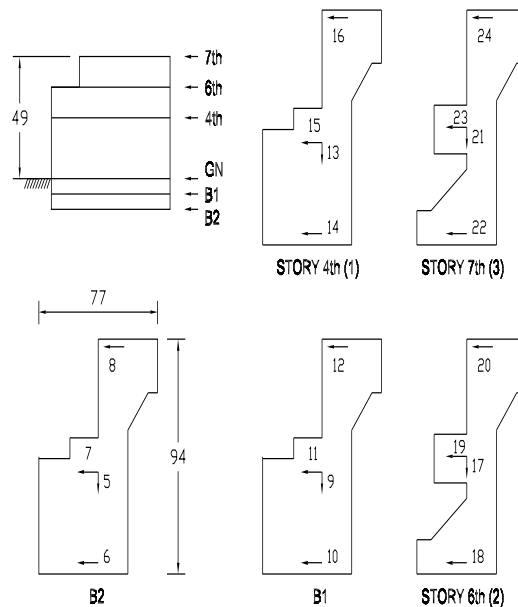


Fig. 10. Scheme of hospital building (dimensions in m).

way to recover torsion terms in the stiffness and damping matrices. Beyond the almost perfect match in acceleration estimation, the only analysis that can be performed with the available acceleration data is to obtain its Fourier transform. However, this spectra can not be directly related to the natural frequencies of the structure as it hides all interaction effects. Processing this data is equivalent to a reduced model estimation of only one degree of freedom, that is insufficient for 3D identification purposes.

VII. CONCLUSION

A least squares identification algorithm for real-time recovering of the parameters of a building elastic model, seismically excited with two orthogonal horizontal components was presented. The parameters were recovered by using measurements of accelerometers arbitrarily arranged on each

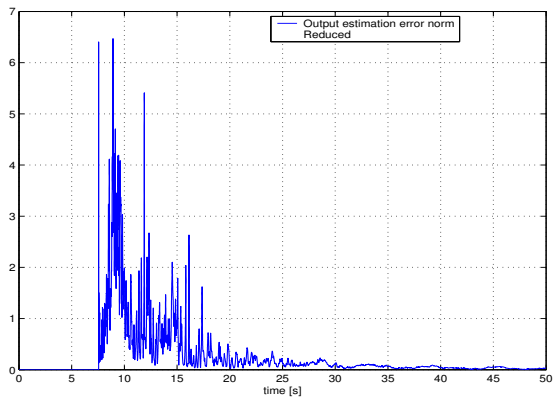


Fig. 11. Hospital building. Output error norm: $\|\varepsilon\|_2$

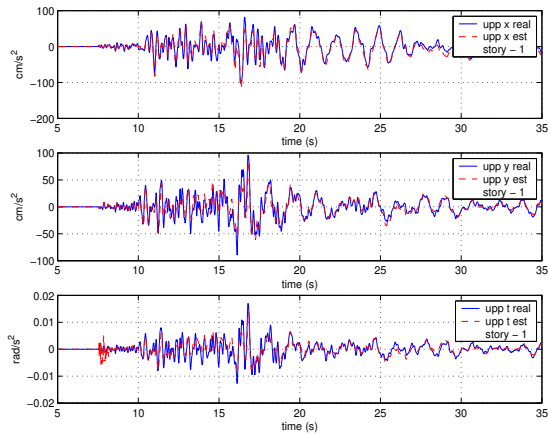


Fig. 12. Hospital building. Measured and estimated accelerations, 1st story.

story. The mathematical model considers 3 DOF for each story, two displacements and one torsion. Simple expressions for recovering the kinematics of the center of mass of each story with the available measurements were found. The least squares algorithm introduced, includes an efficient re-parameterization that greatly improves numerical calculation speed and allows real-time identification. Simulation results show convergence in finite time in the parameter identification process and very good agreement between theoretical and identified natural frequencies, for both full instrumented and partially instrumented buildings. An important finding was the fact that the algorithm allows to recover the center of torsion for each story.

The algorithm was also tested with field data obtained from instrumented buildings. Even though this data was not pre-processed, output convergence was excellent and parameter convergence was good. Experimental work with small scale models and the use of observers to improve velocity and displacement estimation is on-going work.

REFERENCES

[1] J. J. Connor and B. S. A. Klink, *Introduction to motion based design*. Southampton, United Kingdom: Computational Mechanics, 1996.

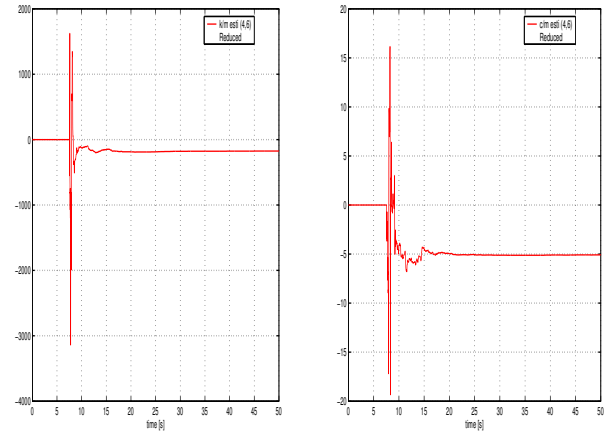


Fig. 13. Hospital building. Time evolution of parameters. (a) element $(M^{-1}K)_{4,6}$. (b) element $(M^{-1}C)_{4,6}$.

TABLE IV
IDENTIFIED FREQUENCIES [rad/s]

E54P	Hospital
1,0594	3,5706
1,2471	6,7722
1,8191	6,9859
3,3465	7,9887
3,5002	10,625
3,7315	12,407
4,5800	15,610
6,5119	18,919
8,0127	
9,4224	
12,0000	

[2] E. Safat, "Detection and identification of soil-structure interaction in buildings from vibration recordings," *ASCE Journal of Structural Engineering*, vol. 121, pp. 899–906, 1995.

[3] Y. Li and S. Mau, "A case of study of mimo system identification applied to building seismic records," *Earthquake Engineering and Structural Dynamics*, vol. 20, pp. 1045–1064, 1991.

[4] J. Stewart and G. Fenves, "System identification for evaluating soil-structure interaction effects in buildings from strong motion recordings," *Earthquake Engineering and Structural Dynamics*, vol. 27, pp. 869–885, 1998.

[5] R. Rodríguez Rocha and L. Barroso, "Método de cocientes de valores de rigidez entre valores de masa para la obtención del estado no dañado de una estructura y detección de daño de la estructura de referencia," in *XVI Congreso Nacional de Ingeniería Sísmica, Guanajuato, México*, 2003.

[6] M. Paz, *Structural Dynamics: theory and computation*, 4th ed. New York, NY: Chapman & Hall, International Thomson Publishing, 1997.

[7] A. Chopra, *Dynamics of Structures: Theory and Applications to Earthquake Engineering*. Upper Saddle River, NJ: Prentice-Hall, 1995.

[8] R. Meli, *Diseño estructural*. Limusa, 1985.

[9] J. Angeles and L. Alvarez-Icaza, "3D identification of a seismically excited building," in *Proceedings of the 16th IFAC World Congress*, Prague, Czech Republic, 2005, pp. Tu-A01-TP/1.

[10] —, "3D identification of a seismically excited building with sensors arbitrarily placed," in *Proceedings of the 2006 American Control Conference*, Minneapolis, USA, 2006, pp. 3807–3812.

[11] Åström, K.J. and Wittenmark, B., *Adaptive Control*, 2nd ed. USA: Addison-Wesley, 1995.

[12] F. Naïm, "Response of instrumented buildings to 1994 northridge earthquake," John A. Martin and Associates, Inc., Tech. Rep., 1994.